Biochemical Pharmacology, Vol. 57, pp. 171–179, 1999.

ISSN 0006-2952/99/$–see front matter
PII S006-2952(98)00277-9

Characterization of the Subtype Selectivity of the Allosteric Modulator Heptane-1,7-bis-(dimethyl-3′-phthalimidopropyl) Ammonium Bromide (C_7/3-phth) at Cloned Muscarinic Acetylcholine Receptors

Arthur Christopoulos, Jennifer L. Sorman,* Fred Mitchelson† and Esam E. El-Fakahany*‡*

*Division of Neuroscience Research in Psychiatry, University of Minnesota Medical School, Minneapolis, MN 55455, U.S.A.; and †Department of Pharmaceutical Biology and Pharmacology, Victorian College of Pharmacy (Monash University), Parkville, 3052, Victoria, Australia

ABSTRACT. The present study investigated the interaction between the muscarinic acetylcholine receptor (mAChR) allosteric modulator heptane-1,7-bis-(dimethyl-3′-phthalimidopropyl) ammonium bromide (C_7/3-phth) and the orthosteric antagonist [^{3}H]*N*-methylscopolamine ([^{3}H]NMS) at the five cloned human mAChRs expressed in Chinese hamster ovary cells. Equilibrium binding studies, using two different concentrations of radioligand, showed the interaction between C_7/3-phth and [^{3}H]NMS to be characterized by different degrees of negative cooperativity, depending on the receptor subtype. The modulator exhibited the highest affinity (85 nM) for the unoccupied M_2 receptor and the lowest affinity for the unoccupied M_5 receptor, the latter being approximately 100-fold lower. In contrast, the highest degree of negative cooperativity was observed at the M_5 receptor, whereas lowest negative cooperativity was found at the M_1 and M_4 receptors. Non-equilibrium dissociation kinetic studies also confirmed the allosteric properties of C_7/3-phth at all five mAChRs and yielded independent estimates of the modulator affinity for the occupied receptor. The latter estimates showed good agreement with those calculated using parameter values determined from the equilibrium experiments. The present results extend previous findings that C_7/3-phth is a potent allosteric modulator at mAChRs, particularly the M_2 subtype, and also highlight the effects of cooperativity on apparent drug–receptor subtype selectivity. BIOCHEM PHARMACOL **57**;2:171–179, 1999. © 1998 Elsevier Science Inc.

KEY WORDS. muscarinic receptors; allosteric modulation; equilibrium binding; dissociation kinetics; cooperativity

The five known subtypes of mAChRs§ exhibit a marked degree of sequence similarity, particularly with respect to domains comprising the classic, orthosteric, binding site recognized by agonists, such as acetylcholine, and competitive antagonists, such as atropine [1, 2]. The development of pharmacotherapeutic agents targeted to this binding site and able to discriminate effectively between subtypes has thus remained relatively elusive. An alternative approach may be to exploit the secondary, allosteric, binding site known to be located on the mAChRs [3–6]. This site is comprised of ligand attachment points that are, necessarily, different from those located within the orthosteric binding domain and probably show greater diversity between mAChR subtypes [5, 7].

In radioligand binding studies, allosteric modulation is commonly manifested either as a change in radioligand dissociation characteristics, or as a deviation of radioligand binding isotherms from classical, Langmuirian behavior at equilibrium [3]. When employed in tandem, both equilibrium and kinetic approaches should yield complementary information with regard to the quantitation of the parameters describing the allosteric interaction; namely, the affinity of the modulator for the allosteric binding site and the cooperativity of the interaction when both orthosteric and allosteric sites are occupied simultaneously [7, 8].

C_7/3-phth (Fig. 1) has been identified as one of the most potent allosteric modulators of ligand binding at M_2 mAChRs [9–11]. In addition, allosteric properties of this ligand have been identified at some other mAChR subtypes [9, 12]. However, all studies using this compound have, to date, been conducted on native mAChRs expressed in various tissues [9–17], which often contain a mixture of mAChRs. To obtain a clearer and more complete quanti-

‡ Corresponding Author: Prof. Esam E. El-Fakahany, Neuroscience Research in Psychiatry, Box 392, Mayo Memorial, University of Minnesota Medical School, Minneapolis, MN 55455. Tel. (612) 624 8432; FAX: (612) 624 8935; E-mail: elfak001@maroon.tc.umn.edu

§ *Abbreviations:* CHO, Chinese hamster ovary; C_7/3-phth, heptane-1,7-bis-(dimethyl-3′-phthalimidopropyl) ammonium bromide; DMEM, Dulbecco's modified Eagle's medium; mAChR, muscarinic acetylcholine receptor; and NMS, *N*-methylscopolamine.

Received 28 April 1998; accepted 15 July 1998.

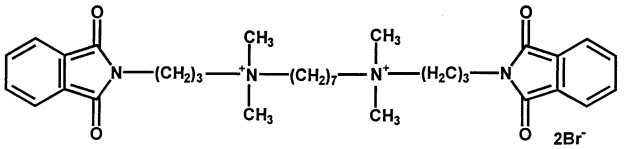

FIG. 1. Structure of C_7/3-phth.

tative description of the binding properties of C_7/3-phth at various mAChRs, the present study has investigated the interaction between this compound and the orthosteric antagonist [^{3}H]NMS at the individual M_1–M_5 mAChR subtypes expressed in CHO cells.

MATERIALS AND METHODS

Materials

[^{3}H]NMS (84.5 Ci/mmol) was obtained from NEN Dupont; C_7/3-phth was synthesized by the Institute of Drug Technology; DMEM was purchased from GIBCO; geneticin from Calbiochem; bovine calf serum from HyClone; and atropine sulfate from the Sigma Chemical Co.

Cell Culture

CHO cells, stably expressing the human M_1–M_5 mAChRs, were provided by Dr. M. Brann (University of Vermont Medical School) and were grown for 4 days at 37° in DMEM, supplemented with 10% bovine calf serum and 50 μg/mL of geneticin, in a humidified atmosphere consisting of 5% CO_2 and 95% air.

Membrane Preparation

Cells were harvested by trypsinization 4 days after subculture, and centrifuged (300 *g*, 3 min) before resuspension of the pellet in phosphate buffer (50 mM Na_2HPO_4, pH 7.4). Then the cells were homogenized with an Ultra-Turrax (2 × 10 sec bursts, with a 30-sec period of cooling on ice between homogenizations) and centrifuged at 1000 *g* for 10 min. The resulting supernatant was collected and centrifuged at 30,000 *g* for 30 min, after which the pellet was resuspended and immediately used in the binding assays.

Saturation Binding Experiments

All equilibrium radioligand binding experiments used 0.2 mL of homogenate (10–50 μg protein) in a total volume of 1 mL phosphate buffer. For the saturation binding assays, membranes were incubated with increasing concentrations of [^{3}H]NMS (0.02 to 2 nM) for 1 hr at 37° before termination. Non-specific binding was defined using 10 μM atropine. Protein determinations were performed using the method of Bradford [18] with BSA as the standard.

Equilibrium Inhibition Binding Experiments

CHO cell membranes were incubated with a fixed concentration of [^{3}H]NMS, in the absence or presence of increasing concentrations of C_7/3-phth (1 nM–1 mM), added simultaneously with the radioligand, for 1 hr at 37°. Each experiment used a two-curve assay [19], where the fixed concentration of radioligand was 0.2 nM (*ca.* K_D) for the first inhibition curve and 2 nM (*ca.* 10× K_D) for the second inhibition curve. Non-specific binding was defined as above.

Dissociation Kinetic Experiments

A high concentration of membranes (*ca.* 2 mg protein/mL) was incubated with 5 nM [^{3}H]NMS for 1 hr at 37°. Subsequently, 20-μL aliquots were distributed to tubes containing 1 μM atropine in a total volume of 1 mL phosphate buffer to ensure maximal dissociation. Experiments were repeated in the presence of increasing concentrations of C_7/3-phth. The amount of radioactivity was measured at various time intervals to determine the [^{3}H]NMS dissociation rate. Non-specific binding was defined as above. In these experiments, complete dissociation curves were only established for [^{3}H]NMS in the absence or presence of the highest concentration of modulator applied. For radioligand dissociation measured in the presence of intermediate modulator concentrations, a "two-point kinetic" approach was employed [8], whereby radioligand binding was measured at the onset of dissociation and at a single intermediate time point (see Results). This approach is valid if radioligand dissociation curves remain monophasic in the presence of modulator (see Data Analysis).

For all binding experiments, incubation was terminated by filtration through Whatman GF/B filters, positioned on a Brandell Cell Harvester. Filters were washed three times with 4-mL aliquots of ice-cold saline and dried before radioactivity was measured using liquid scintillation counting.

Data Analysis

Data sets of total and non-specific binding, derived from each complete saturation binding assay, were analyzed simultaneously via non-linear regression with ORIGIN 5.0 (Microcal) to derive individual estimates of B_{max} (total receptor density) and K_D (radioligand-receptor equilibrium dissociation constant).

For the equilibrium inhibition binding data, ORIGIN was used to simultaneously analyze both inhibition curves, obtained from each experiment, based on the following equation for allosteric interaction [20]:

$$\frac{Y}{Y_{MAX}} = \frac{[A]}{[A] + K_A \cdot \left(\frac{K_Z + [Z]}{K_Z + [Z]/\alpha}\right)} \quad (1)$$

where Y/Y_{MAX} represents fractional receptor occupancy, [A] and [Z] represent the concentrations, K_A and K_Z represent the equilibrium dissociation constants of the radioligand and allosteric modulator for the unoccupied receptor, respectively, and α represents the heterotropic cooperativity factor between the two ligands. This latter value is a quantitative estimate of the magnitude by which the binding of one ligand to its site on the receptor alters the affinity of the other ligand and vice-versa. Values of $\alpha < 1$ denote positive cooperativity, whereas values of $\alpha > 1$ denote negative cooperativity [20]. The values of [A], [Z], and K_A were entered, and α and K_Z were estimated, as logarithms.

For the non-equilibrium dissociation kinetic experiments, complete dissociation curves for the radioligand, in the absence and presence of the highest concentration of applied modulator, were analyzed initially by nonlinear regression according to mono- and biexponential decay functions. In all cases, curves were adequately described by a monoexponential function, implying fast binding kinetics for C_7/3-phth relative to [^{3}H]NMS [7]. Under these conditions, it is valid to simultaneously fit each complete family of dissociation curves, to the following equation:

$$B_t = B_0 \cdot e^{-k_{off_{obs}} \cdot t} \quad (2)$$

where:

$$k_{off_{obs}} = \frac{[Z]^s \cdot k_{off_Z}/\alpha \cdot K_Z + k_{off}}{1 + [Z]^s/\alpha \cdot K_Z} \quad (3)$$

In the above equations, B_t denotes bound radioligand at time t after dissociation has started, B_0 denotes bound radioligand at equilibrium, $k_{off_{obs}}$ denotes the observed radioligand dissociation constant, k_{off} denotes the rate constant for dissociation of the radioligand from the free (unoccupied) receptor, k_{off_Z} is the rate constant for dissociation of the radioligand from the (modulator) occupied receptor, and $\alpha \cdot K_Z$ is the dissociation constant of the modulator for the (radioligand) occupied receptor. The parameter, *s*, is a slope factor representing the molecularity of the interaction between ligand Z and the receptor. A value of *s* not significantly different from unity may be taken as presumptive evidence of a simple, one-to-one, mass-action relationship between the allosteric modulator and its binding site on the receptor. Apart from the inclusion of the parameter, *s*, in the present formulation, the above equations are formally identical to those derived previously by Lazareno and Birdsall [7].

Data shown are means ± SEM. Comparisons between means were by unpaired *t* tests, or one-way ANOVA as appropriate. Unless otherwise stated, values of $P < 0.05$ were taken as significant.

TABLE 1. Saturation binding parameters for [^{3}H]NMS at cloned human mAChRs in CHO cell membranes

Subtype	Log K_D*	B_{max}† (fmol/mg protein)	N‡
M_1	−9.59 ± 0.16	672 ± 387	5
M_2	−9.81 ± 0.09	385 ± 101	3
M_3	−9.79 ± 0.05	531 ± 89	3
M_4	−9.59 ± 0.08	3322 ± 1005	3
M_5	−9.69 ± 0.03	451 ± 158	3

*Logarithm of the equilibrium dissociation constant, determined by simultaneous nonlinear regression analysis of total and non-specific binding data sets for each experiment. Data represent means ± SEM.

†Total receptor density. Data represent means ± SEM.

‡Number of experiments.

RESULTS

Characterization of the Equilibrium Binding Parameters of [^{3}H]NMS and C_7/3-phth

The binding parameters of [^{3}H]NMS at the five mAChR subtypes in isolated membranes of CHO cells are summarized in Table 1. It may be seen that the affinity of the radioligand was very similar at all five subtypes, whereas estimates of total receptor density showed marked variation.

C_7/3-phth inhibited the equilibrium binding of [^{3}H]NMS at all five mAChRs in a concentration-dependent manner (Figs. 2 and 3). In all instances, the inhibitor displayed an inability to fully abolish radioligand binding, being most pronounced when a high (2 nM) concentration of radioligand was employed. The lower asymptotes of the inhibition binding isotherms reached a plateau at different levels of specific binding across the subtypes, indicative of varying degrees of negative cooperativity [20], and were lowest for the M_3 (Fig. 2B), M_5 (Fig. 2C), and M_2 (Fig. 3A) mAChRs.

A simultaneous analysis of each pair of inhibition curves, obtained at each subtype, according to an allosteric ternary complex model of interaction (Equation 1) yielded parameter estimates for the affinity of the modulator at the free receptor, and the degree of negative cooperativity characterizing the interaction between the modulator and [^{3}H]NMS (Table 2). In agreement with previous observations at native receptors [9, 12], C_7/3-phth demonstrated the highest affinity (85 nM) for the M_2 mAChR (Table 2). The affinity for this subtype was 10-fold higher than for the M_1 mAChR, whereas 20- to 100-fold lower affinities were found for the M_3-M_5 subtypes.

The ability of C_7/3-phth to modulate [^{3}H]NMS binding affinity, and vice versa, is reflected in the value of the cooperativity factor, α. It may be seen in Table 2 that the highest degree of negative cooperativity was manifested at the M_5 receptor, although comparable α values were also observed at the M_2 and M_3 subtypes. In contrast, the allosteric interaction at the M_1 and M_4 mAChRs was characterized by lower degrees of negative cooperativity. No correlation was found between the affinity of C_7/3-phth

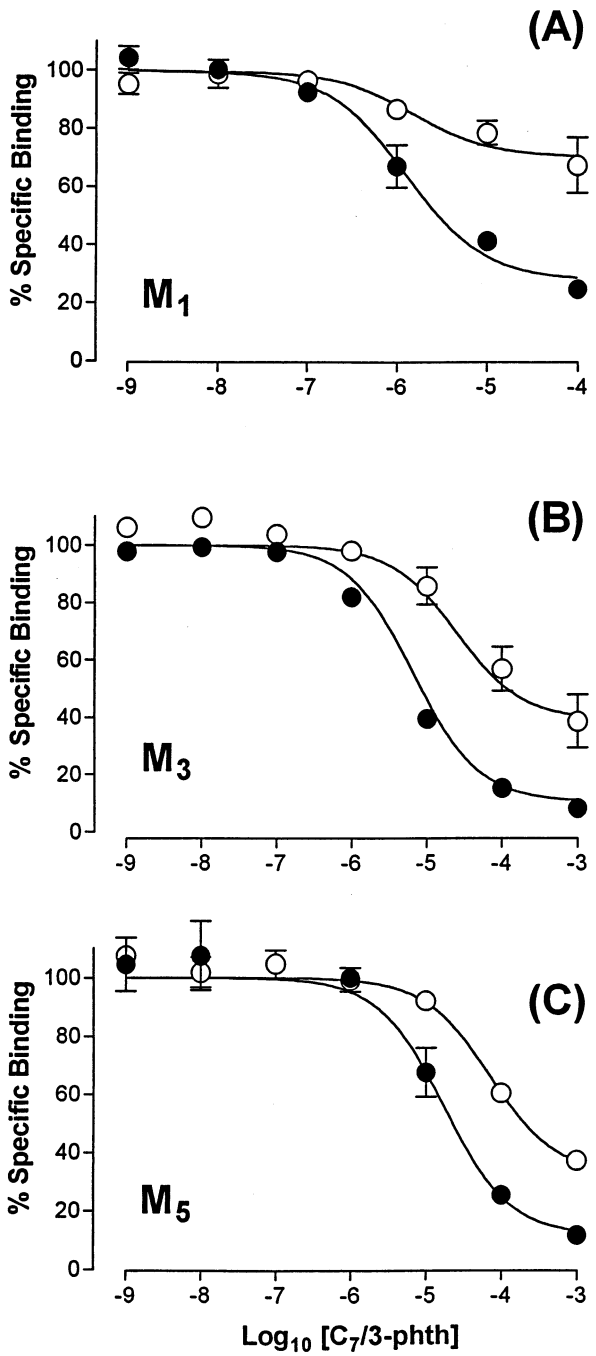

FIG. 2. Effect of C_7/3-phth on the equilibrium binding of [^{3}H]NMS [0.2 nM (●) or 2 nM (○)] in CHO membranes expressing the M_1 (A), M_3 (B), or M_5 (C) mAChRs. Membranes were incubated with both drugs, added simultaneously, in 50 mM phosphate buffer, pH 7.4, at 37° for 1 hr. Normalized curves represent the best fit via constrained, simultaneous nonlinear regression analysis according to an allosteric ternary complex model (see Equation 1 in Data Analysis). Radioligand affinity was determined separately (Table 1) and fixed in the present analysis. Estimated parameter values for the curve fits are shown in Table 2. Points represent the means ± SEM of 3 experiments conducted in duplicate. Where error bars are not shown, they lie within the dimensions of the symbol.

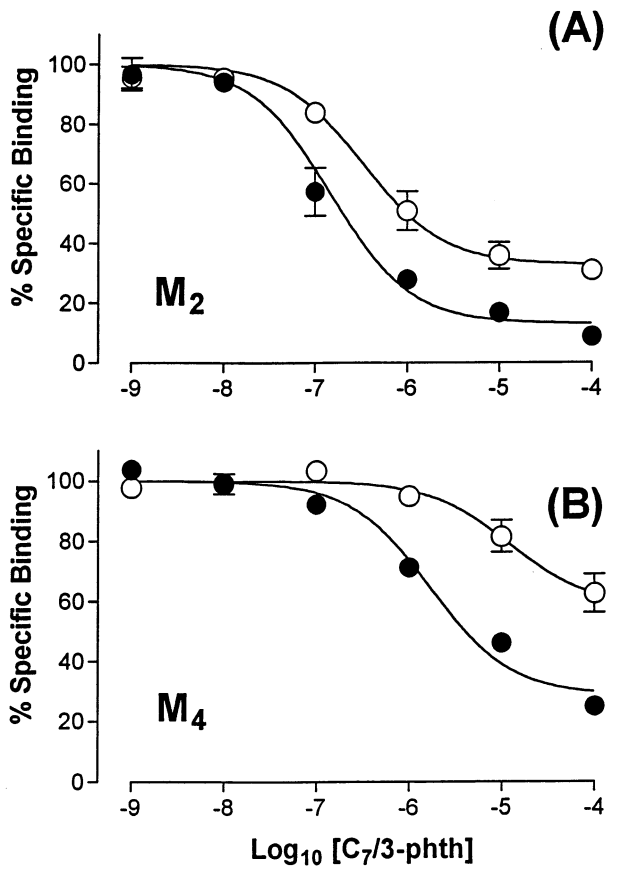

FIG. 3. Effect of C_7/3-phth on the equilibrium binding of [^{3}H]NMS [0.2 nM (●) or 2 nM (○)] in CHO membranes expressing the M_2 (A) or M_4 (B) mAChRs. All other details are as for Fig. 2.

for the free receptors and the cooperativity factors (r^2 = 0.01; $P > 0.05$).

Characterization of the Binding Parameters of C_7/3-phth from a Non-equilibrium Dissociation Kinetic Assay

C_7/3-phth produced a concentration-dependent retardation of [^{3}H]NMS dissociation at all five mAChRs (Figs. 4

TABLE 2. Inhibition binding parameters for C_7/3-phth against [^{3}H]NMS at cloned human mAChRs in CHO cell membranes, determined using an equilibrium binding assay

Subtype	Log K_Z*	Log α†
M_1	−6.07 ± 0.17	0.71 ± 0.07 (5.1)
M_2	−7.07 ± 0.19	1.15 ± 0.02 (14.1)
M_3	−5.45 ± 0.05	1.11 ± 0.09 (12.9)
M_4	−5.79 ± 0.05	0.74 ± 0.05 (5.5)
M_5	−5.03 ± 0.27	1.21 ± 0.07 (16.2)

*Logarithm of the equilibrium dissociation constant for the modulator at the free receptor, estimated by simultaneous nonlinear regression analysis of each pair of inhibition binding isotherms obtained against two different concentrations of radioligand. Data represent means ± SEM of 3 experiments.

†Logarithm of the cooperativity factor. Antilogarithm (geometric mean) is given in parentheses. Data represent means ± SEM of 3 experiments.

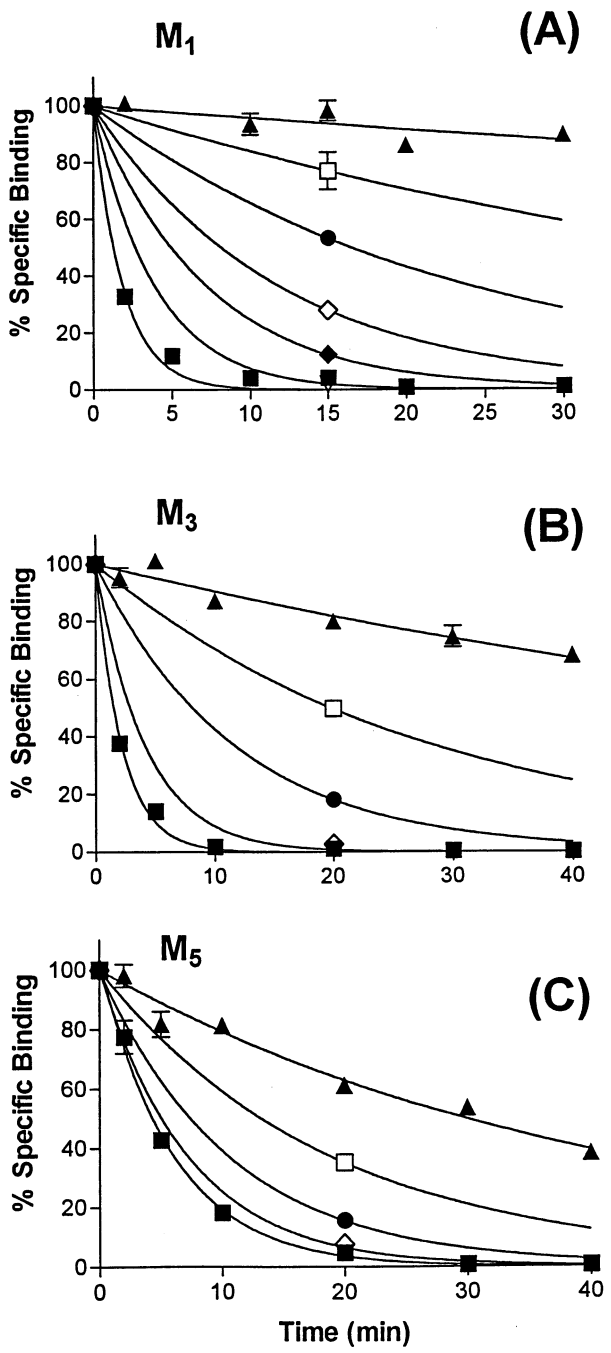

FIG. 4. Effect of C_7/3-phth on the dissociation rate of [^{3}H]NMS in CHO membranes expressing the M_1 (A), M_3 (B), or M_5 (C) mAChRs. Membranes were incubated with 5 nM [^{3}H]NMS at 37° for 1 hr in 50 mM phosphate buffer, pH 7.4, before dissociation was revealed by distribution of membrane aliquots to separate tubes containing 1 μM atropine alone (■) or in combination with C_7/3-phth 3 μM (▽), 10 μM (◆), 30 μM (◇), 0.1 mM (●), 0.3 mM (□) or 1 mM (▲). Normalized curves represent the best fit via constrained, simultaneous nonlinear regression analysis according to Equations 2 and 3 in Data Analysis. The parameter, k_{off_Z} (Equation 3), was not significantly different from zero, and was constrained as such. All other parameter values are listed in Table 3. Points are the means ± range from a single, representative, experiment, conducted in duplicate.

and 5). The dissociation curves for the radioligand in the absence and presence of the highest concentration of modulator were monophasic in all cases, thus, the effects of intermediate concentrations of C_7/3-phth on the apparent radioligand dissociation rate were assessed using a two-point experimental design [8].

A constrained, simultaneous analysis of each complete family of curves observed per subtype per experiment, according to Equations 2 and 3 in Data Analysis, yielded the parameters listed in Table 3. The dissociation rate constant (k_{off}) of [^{3}H]NMS at 37°, measured in the absence of modulator, showed a greater diversity in magnitude across the subtypes, in contrast to the K_D (cf. Table 1). This latter finding is not unusual, however, as previous studies have also reported such deviations in [^{3}H]NMS dissociation rates across the five mAChR subtypes [4, 21, 22]. Dissociation was fastest at the M_2 receptor, the k_{off} being *ca.* 7-fold greater than at the M_5 receptor. In Equation 3 (Data

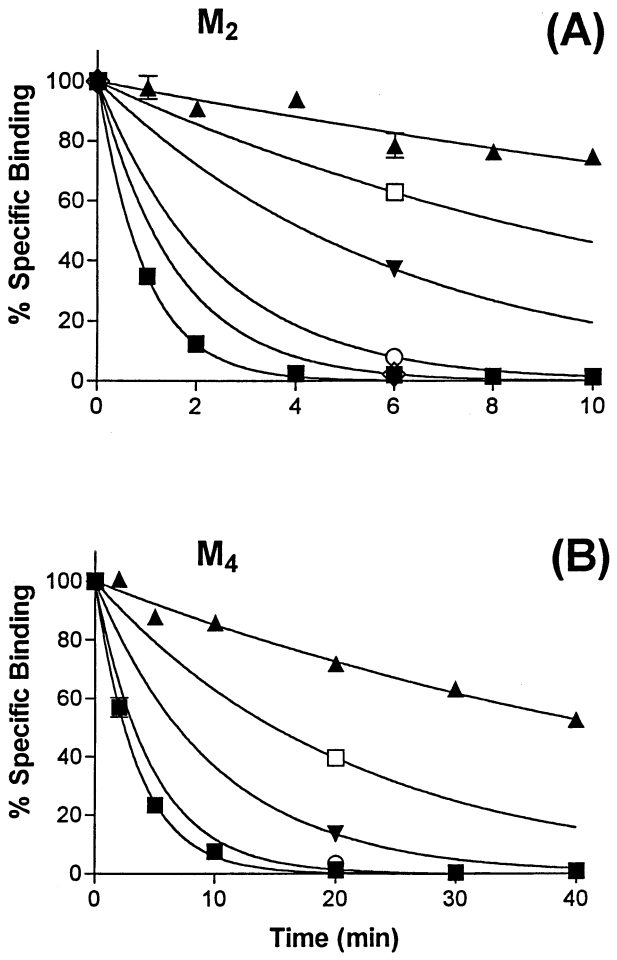

FIG. 5. Effect of C_7/3-phth on the dissociation rate of [^{3}H]NMS in CHO membranes expressing the M_2 (A) or M_4 (B) mAChRs. Membranes were incubated with 5 nM [^{3}H]NMS at 37° for 1 hr in 50 mM phosphate buffer, pH 7.4, before dissociation was revealed by distribution of 20-μL aliquots to separate tubes containing 1 μM atropine alone (■) or in combination with C_7/3-phth 1 μM (◇), 3 μM (○), 10 μM (▼), 30 μM (□) or 0.1 mM (▲). All other details are as for Fig. 4.

TABLE 3. Dissociation rate constant parameters for [^{3}H]NMS and dissociation constants for C_7/3-phth at cloned human mAChRs in CHO cell membranes, determined using a non-equilibrium kinetic assay

Subtype	k_{off}* (min^{-1})	Log $\alpha \cdot K_Z$†		s‖	N¶
		Obs.‡	Calc.§		
M_1	0.47 ± 0.03	−5.09 ± 0.07	−5.36	0.88 ± 0.15	5
M_2	1.52 ± 0.15	−5.99 ± 0.30	−5.92	0.98 ± 0.15	5
M_3	0.39 ± 0.02	−4.38 ± 0.09	−4.34	1.02 ± 0.12	4
M_4	0.34 ± 0.02	−5.61 ± 0.19	−5.06	0.97 ± 0.10	5
M_5	0.23 ± 0.06	−3.82 ± 0.06	−3.83	0.95 ± 0.25	4

*Dissociation rate constant of [^{3}H]NMS at the unoccupied receptor, determined by simultaneous nonlinear regression analysis of all radioligand dissociation curves, in the absence or presence of various concentrations of C_7/3-phth, according to Equations 2 and 3. The value for k_{off_Z} (Equation 3) was not significantly different from 0 in all cases. Data represent means ± SEM.

†Logarithm of the dissociation constant of C_7/3-phth at the [^{3}H]NMS-occupied receptor.

‡Determined by simultaneous nonlinear regression analysis according to Equations 2 and 3, with the slope factor, *s*, constrained to unity. Data represent means ± SEM.

§Calculated by multiplying the dissociation constant of C_7/3-phth at the free receptor by the cooperativity factor, derived from the equilibrium assays and shown in Table 2.

‖Slope factor, according to Equation 3. None of the values were significantly different from 1. Data represent means ± SEM.

¶Number of experiments.

Analysis), the parameter k_{off_Z} reflects the radioligand dissociation rate constant for the modulator-bound receptor. In all analyses, this latter parameter was found to be not significantly different from zero ($P > 0.05$), and was constrained as such. This finding is consistent with C_7/3-phth being able to completely prevent [^{3}H]NMS dissociation from mAChRs. The values for the slope factor, *s*, in Equation 3 were not significantly different from unity ($P > 0.05$), implying a simple mass-action relationship between C_7/3-phth and the allosteric binding site.

Also listed in Table 3 are the estimates of the affinity of C_7/3-phth for the occupied receptors, as determined from the kinetic assays. The values listed in the Table are from analyses according to Equations 2 and 3, but with the slope parameter, s, constrained to 1. Theoretically, the modulator affinity for the occupied receptor should correspond to the product of the modulator affinity for the free receptor and the cooperativity factor [4]. For comparison, the values of these latter parameters, determined in the equilibrium binding assays, were used to calculate theoretical values for $\alpha \cdot K_Z$, and were included in Table 3. It may be seen that, overall, a good concordance was found between the values determined from both types of assays.

DISCUSSION

Ligands that are able to regulate mAChR function via an allosteric mechanism represent some of the most subtype-selective agents for these receptors [6]. This observation highlights the fact that allosteric modulators interact with regions of the receptor that probably do not show the strong sequence conservation associated with the orthosteric site [7]. The design of effective therapeutic agents exploiting the allosteric sites present on the mAChRs requires the identification of potent pharmacological probes for these sites, as well as the quantitation of the interaction between such probes and the mAChRs. C_7/3-phth is one such agent, and is representative of a class of alkane-bis-ammonium compounds that have proven to be very useful lead compounds in the search for structure-activity relationships among mAChR allosteric modulators [10, 11, 13]. In fact, at the M_2 mAChR, Tränkle *et al.* [10] found this compound to rank second only to alcuronium, a prototypical allosteric modulator [5, 23], in terms of its ability to decelerate [^{3}H]NMS dissociation.

In the present study, the ability of C_7/3-phth to modulate [^{3}H]NMS binding at all five mAChRs has been confirmed and quantitated. Analysis of the equilibrium binding isotherms according to an allosteric ternary complex model [20] allowed for the determination of the affinity of C_7/3-phth for the unoccupied receptor and the cooperativity factor characterizing the interaction between this ligand and [^{3}H]NMS at the receptor. The results in Figs. 2 and 3, and in Table 2, indicated that C_7/3-phth possesses highest affinity for the M_2 mAChR, in agreement with previous studies on native receptors [9, 12, 15]. The preferential selectivity of C_7/3-phth for this latter subtype is also in accord with the observation that many positively charged allosteric modulators of mAChRs have a high affinity for the M_2 mAChR [6, 24, 25]. Indeed, a recent study by Tränkle *et al.* [25] has lent further credence to the hypothesis that certain M_2-selective antagonists may utilize domains associated with the allosteric site in their interaction with the receptor protein. However, the ability of C_7/3-phth to modulate [^{3}H]NMS binding at the five mAChRs also supports studies demonstrating the existence of allosteric interactions at all of the mAChR subtypes [24, 26, 27].

The lack of correlation between the affinity of C_7/3-phth for the free mAChRs and the cooperativity factors for the interaction between the modulator and [^{3}H]NMS highlights the complex nature of allosteric modulation. Unlike orthosteric interactions, allosteric interactions are characterized by *two* unconditional dissociation constants (K_A and K_Z) *and* a cooperativity factor (α) [3]. The latter is highly dependent on the nature of the ligands occupying the two sites [28], and thus it is not possible to predict the effects of a particular modulator on the binding of one orthosteric ligand based on information derived using another. Furthermore, high negative cooperativity may appear indistinguishable from orthosteric competition in equilibrium binding experiments [20]. For example, previous experiments with C_7/3-phth against the binding of the antagonist [^{3}H]quinuclidinyl benzilate in rat cortex yielded inhibition curves that could be fitted adequately to a two-site competitive binding model [12]. In the present study, the binding isotherms obtained with C_7/3-phth against 0.2 nM [^{3}H]NMS at the M_2, M_3, and M_5 mAChRs, if analyzed independently, may also be misinterpreted as

examples of a competitive interaction. Increasing the concentration of radioligand 10-fold, however, allowed the allosteric nature of the interaction to be readily visualized. Additionally, this type of two-curve experimental design possesses analytical advantages, since a constrained, simultaneous analysis of each curve pair increases the degrees of freedom and allows for more accurate parameter estimates than experiments utilizing single curves for each assay [29].

The experiments outlined above were conducted at equilibrium, and thus reflect the steady-state effects of an allosteric modulator on both radioligand association and dissociation [8, 10]. Although a competitive interaction at the orthosteric site may also yield apparent reductions in radioligand association, a change in the dissociation characteristics of a drug–receptor pair in the presence of another ligand is a hallmark of allosteric modulation [6, 8]. Thus, an alternative approach that has proven popular in the detection of allosterism has been the use of non-equilibrium, dissociation kinetic assays. Furthermore, dissociation kinetic assays may be analyzed in a quantitative fashion to derive the affinity of the modulator for the occupied receptor and the maximal effect on radioligand dissociation [7, 8, 30]. Accordingly, C_7/3-phth was found to retard the dissociation of [^{3}H]NMS at the M_1–M_5 mAChRs in a concentration-dependent manner (Figs. 4 and 5), again confirming its allosteric properties at all five mAChR subtypes. Additionally, the estimates of modulator affinity for the [^{3}H]NMS-occupied receptor (Table 3) showed good agreement with the theoretical values predicted from the equilibrium binding experiments, although some discrepancy was noted for the M_1 and M_4 mAChRs. Although probably not significant, the finding may be indicative of a slightly different mode of interaction between C_7/3-phth and the occupied, compared with the unoccupied, M_1 and M_4 receptors.

The approach used in the present study to quantitate the kinetic experiments was based on a method outlined by Lazareno and Birdsall [7], whereby the entire family of curves obtained in each individual experiment are subject to a constrained, simultaneous nonlinear regression analysis in order to obtain the relevant model parameters. The application of a quantitative approach to the analysis of allosterism in dissociation kinetic experiments, however, was originally demonstrated by Ellis and Seidenberg [30]. In their elegant approach, the apparent radioligand dissociation rate constants in the presence of modulator (i.e. $k_{off_{obs}}$), were converted to fractions of the control rate constant (k_{off}) and fitted to a logistic function in order to derive estimates of the modulator affinity for the occupied receptor (K_{app}) and the maximal effect (m) of the modulator on radioligand dissociation. It should be noted that both approaches are equivalent, as $K_{app} = \alpha \cdot K_Z$, and $m = 1 - (k_{off_Z}/k_{off})$.

Although equilibrium experiments are almost invariably employed in the classification of drugs and receptors, kinetic approaches are also valuable, as they often serve as more sensitive indicators of differences among receptor subtypes and have sometimes been used in the receptor classification process [21]. For example, the results in Table 1 indicate that [^{3}H]NMS does not differentiate significantly between subtypes under the assay conditions employed, whereas the rate constants in Table 3 show a greater divergence. In terms of therapeutic usage, the removal of drugs from the receptor compartment of various organs will be influenced by the kinetic characteristics of the ligand–receptor complex, in which case the interaction between the drug and endogenous neurotransmitters under non-equilibrium conditions assumes a paramount importance. Ideally, equilibrium and kinetic approaches should be employed in tandem, and under the same assay conditions. This is important particularly for the study of allosteric interactions, as the latter are especially sensitive to the experimental assay conditions employed [10, 31, 32].

Overall, the combined findings for the interaction between C_7/3-phth and [^{3}H]NMS in both the equilibrium and kinetic assays highlight an important consideration in the design, evaluation, and, ultimately, therapeutic utilization of allosteric modulators; the subtype-selectivity profile for a modulator at the unoccupied receptor may not reflect the observed binding profile at the occupied receptor. The latter will be determined by the cooperativity between orthosteric and allosteric sites, and therefore is dependent on the nature of the ligand occupying each site [3, 6]. This phenomenon may be represented graphically (Fig. 6). The occupancy of C_7/3-phth for the free mAChR, based on the log K_Z values of Table 2, is shown in Fig. 6A, whereas the occupancy of the modulator at the [^{3}H]NMS-bound receptor, based on the experimentally-determined log $\alpha \cdot K_Z$ values in Table 3, is shown in Fig. 6B. The negative cooperativity characterizing the interaction results in a dextral-shift of the modulator-occupancy curves toward lower affinity (Fig. 6B). Even more interesting, however, is the fact that the rank order of affinity may also be altered. This highlights the capricious nature of the cooperativity factor. Thus, the design and utilization of allosteric modulators for therapeutic purposes must take into consideration the simultaneous presence of any orthosteric agents. Such agents may include the endogenous neurotransmitter, acetylcholine [7, 33, 34], as well as any concomitantly administered exogenous agents (e.g. antagonists and synthetic agonists). In this latter regard, it is noteworthy that anti-muscarinic properties have been ascribed to a variety of currently used therapeutic agents [35].

In conclusion, the present study has demonstrated the utility of complementing equilibrium approaches with kinetic studies of allosterism by quantitating the interaction between the modulator, C_7/3-phth, and [^{3}H]NMS at all five mAChR subtypes. This modulator displays the highest affinity for the M_2 mAChR. The present results also highlight how interaction with the occupied receptor can yield a different pattern of apparent affinities that need to be considered when designing and testing modulators for therapeutic usage.

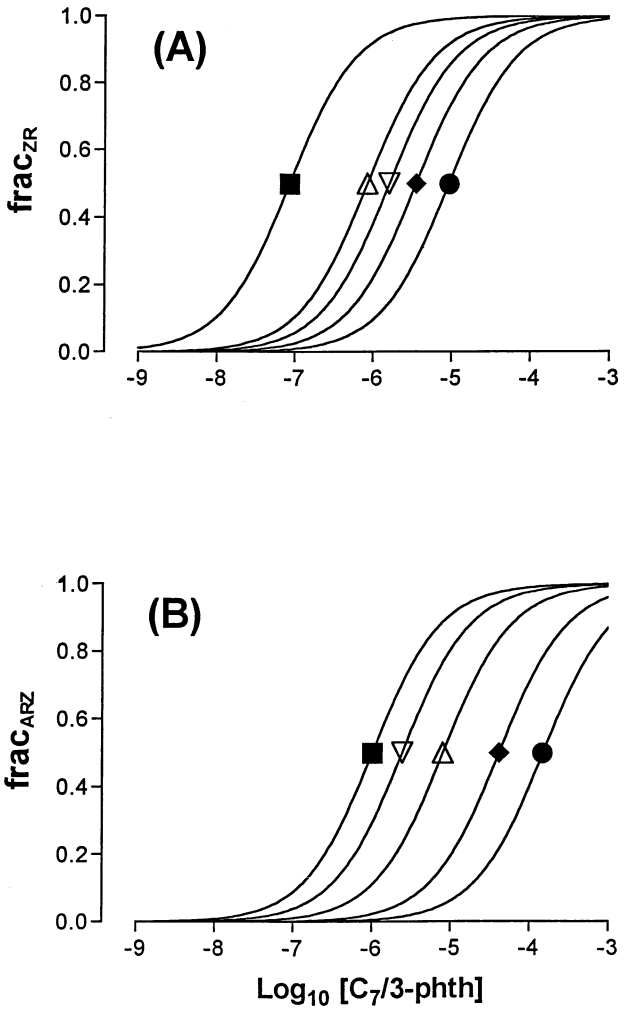

FIG. 6. Theoretical occupancy curves for C_7/3-phth at the M_1 (△), M_2 (■), M_3 (♦), M_4 (▽), and M_5 (●) mAChRs. (A), $frac_{ZR}$ denotes fractional occupancy at the free receptor and is based on the values for Log K_Z determined from equilibrium binding experiments and shown in Table 2. (B), $frac_{ARZ}$ denotes fractional occupancy at the [^{3}H]NMS-occupied receptor and is based on the values for Log $\alpha \cdot K_Z$ determined from the dissociation kinetic experiments and shown in Table 3.

The authors gratefully acknowledge the expert technical assistance of Marianne K. O. Grant. This study was supported by National Institutes of Health Grant NS25743.

References

1. Hulme EC, Birdsall NJM and Buckley NJ, Muscarinic receptor subtypes. *Annu Rev Pharmacol Toxicol* **30:** 633–673, 1990.
2. Wess J, Mutational analysis of muscarinic acetylcholine receptors: Structural basis of ligand/receptor/G protein interactions. *Life Sci* **53:** 1447–1463, 1993.
3. Christopoulos A, Lanzafame A and Mitchelson F, Allosteric interactions at muscarinic cholinoceptors. *Clin Exp Pharmacol Physiol* **25:** 185–194, 1998.
4. Ellis J, Allosteric binding sites on muscarinic receptors. *Drug Dev Res* **40:** 193–204, 1997.
5. Tucek S and Proska J, Allosteric modulation of muscarinic acetylcholine receptors. *Trends Pharmacol Sci* **16:** 205–212, 1995.
6. Lee NH and El-Fakahany EE, Allosteric antagonists of the muscarinic acetylcholine receptor. *Biochem Pharmacol* **42:** 199–205, 1991.
7. Lazareno S and Birdsall NJM, Detection, quantitation, and verification of allosteric interactions of agents with labeled and unlabeled ligands at G protein-coupled receptors: Interactions of strychnine and acetylcholine at muscarinic receptors. *Mol Pharmacol* **48:** 362–378, 1995.
8. Kostenis E and Mohr K, Two-point kinetic experiments to quantify allosteric effects on radioligand dissociation. *Trends Pharmacol Sci* **17:** 280–283, 1996.
9. Christopoulos A and Mitchelson F, Assessment of the allosteric interactions of the bisquaternary heptane-1,7-bis(dimethyl-3′-pthalimidopropyl)ammonium bromide at M_1 and M_2 muscarine receptors. *Mol Pharmacol* **46:** 105–114, 1994.
10. Tränkle C, Kostenis E, Burgmer U and Mohr K, Search for lead structures to develop new allosteric modulators of muscarinic receptors. *J Pharmacol Exp Ther* **279:** 926–933, 1996.
11. Staudt M, Tränkle C, Mohr K and Holzgrabe U, Contribution of lateral substituents in heptane-bisammonium derivatives to the allosteric stabilization of antagonist binding to M_2-receptors. *Life Sci* **62:** 423–429, 1997.
12. Christopoulos A, Loiacono R and Mitchelson F, Binding of the muscarine receptor antagonist heptane-1,7-bis(dimethyl-3′-pthalimidopropyl)ammonium bromide at cholinoceptor sites. *Eur J Pharmacol* **246:** 1–8, 1993.
13. Lüllman H, Ohnesorge FK, Schauwecker G-C and Wasserman O, Inhibition of the actions of carbachol and DFP on guinea pig isolated atria by alkane-bis-ammonium compounds. *Eur J Pharmacol* **6:** 241–247, 1969.
14. Mitchelson F, Antimuscarinic action of an alkane-bis-ammonium compound alone and in combination with (+)-benzetimide. *Eur J Pharmacol* **33:** 237–246, 1975.
15. Choo LK and Mitchelson F, Characterization of the antimuscarinic effect of heptane-1,7-bis-(dimethyl-3′-phthalimidopropyl ammonium bromide). *Eur J Pharmacol* **162:** 429–435, 1989.
16. Lanzafame A, Christopoulos A and Mitchelson F, Interactions of agonists with an allosteric antagonist at muscarinic acetylcholine M_2 receptors. *Eur J Pharmacol* **316:** 27–32, 1996.
17. Lanzafame A, Christopoulos A and Mitchelson F, Three allosteric modulators act at a common site, distinct from that of competitive antagonists, at muscarinic acetylcholine M_2 receptors. *J Pharmacol Exp Ther* **282:** 278–285, 1997.
18. Bradford MM, A rapid and sensitive method for the quantitation of microgram quantities of protein utilizing the principle of protein-dye binding. *Anal Biochem* **72:** 248–254, 1976.
19. Christopoulos A, Lanzafame A, Ziegler A and Mitchelson F, Kinetic studies of co-operativity at atrial muscarinic M_2 receptors with an "infinite dilution" procedure. *Biochem Pharmacol* **53:** 795–800, 1997.
20. Ehlert FJ, Estimation of the affinities of allosteric ligands using radioligand binding and pharmacological null methods. *Mol Pharmacol* **33:** 187–194, 1988.
21. Waelbroeck M, Tastenoy M, Camus J and Christophe J, Binding of selective antagonists to four muscarinic receptors (M_1 to M_4) in rat forebrain. *Mol Pharmacol* **38:** 267–273, 1990.
22. Flynn DD, Reever CM and Ferrari-DiLeo, G, Pharmacological strategies to selectively label and localize muscarinic receptor subtypes. *Drug Dev Res* **40:** 104–116, 1997.
23. Tucek S, Musilkova J, Nedoma J, Proska J, Shelkvnikov S and Vorlicek J, Positive cooperativity in the binding of alcuronium and *N*-methylscopolamine to muscarinic acetylcholine receptors. *Mol Pharmacol* **38:** 674–680, 1990.
24. Ellis J, Huyler J and Brann MR, Allosteric regulation of

cloned m1–m5 muscarinic receptor subtypes. *Biochem Pharmacol* **42:** 1927–1932, 1991.
25. Tränkle C, Andresen I, Lambrecht G and Mohr K, M_2 receptor binding of the selective antagonist AF-DX 384: Possible involvement of the common allosteric site. *Mol Pharmacol* **53:** 304–312, 1998.
26. Jakubík J, Bacáková L, El-Fakahany EE and Tucek S, Subtype selectivity of the positive allosteric action of alcuronium at cloned M_1–M_5 muscarinic acetylcholine receptors. *J Pharmacol Exp Ther* **274:** 1077–1083, 1995.
27. Lazareno S, Gharagozloo P, Kuonen D, Popham A and Birdsall NJM, Subtype-selective positive cooperative interactions between brucine analogs and acetylcholine at muscarinic recptors: Radioligand binding studies. *Mol Pharmacol* **53:** 573–589, 1998.
28. Lee NH and El-Fakahany EE, Influence of ligand choice on the apparent binding profile of gallamine to cardiac muscarinic receptors. Identification of three main types of gallamine-muscarinic receptor interactions. *J Pharmacol Exp Ther* **246:** 829–838, 1988.
29. Leff P, Prentice DJ, Giles H, Martin GR and Wood J, Estimation of agonist affinity and efficacy by direct, operational model-fitting. *J Pharmacol Methods* **23:** 225–237, 1990.
30. Ellis J and Seidenberg M, Two allosteric modulators interact at a common site on cardiac muscarinic receptors. *Mol Pharmacol* **42:** 638–641, 1992.
31. Pedder EK, Eveleigh P, Poyner D, Hulme EC and Birdsall NJM, Modulation of the structure-binding relationships of antagonists for muscarinic acetylcholine receptor subtypes. *Br J Pharmacol* **103:** 1561–1567, 1991.
32. Waelbroeck M, Identification of drugs competing with *d*-tubocurarine for an allosteric site on cardiac muscarinic receptors. *Mol Pharmacol* **46:** 685–692, 1994.
33. Gnagey A and Ellis J, Allosteric regulation of the binding of [^{3}H]acetylcholine to m2 muscarinic receptors. *Biochem Pharmacol* **52:** 1767–1775, 1996.
34. Jakubík, J, Bacakova L, El-Fakahany EE and Tucek S, Positive cooperativity of acetylcholine and other agonists with allosteric ligands on muscarinic acetylcholine receptors. *Mol Pharmacol* **52:** 172–179, 1997.
35. Richelson E, Are receptor studies useful for clinical practice? *J Clin Psychiatry* **44:** 4–9, 1983.